PHENIX and the Reaction Plane: Recent Results

David L. Winter, for the PHENIX Collaboration [1]

Columbia University, NY, NY 10027

E-mail: winter@nevis.columbia.edu

Abstract. During the past several years, experiments at RHIC have established that a dense partonic medium is produced in Au+Au collisions at $\sqrt{s} = 200$ GeV. Subsequently, a primary goal of analysis has been to understand and characterize the dynamics underlying this new form of matter. Among the many probes available, the measurements with respect to the reaction plane have proven to be crucial to our understanding of a wide range of topics, from the hydrodynamics of the initial expansion of the collision region to high-$p_{\rm T}$ jet quenching phenomena. Few tools have the ability to shed light on such a wide variety of observables as the reacion plane. In this talk, we discuss recent PHENIX measurements with respect to the reaction plane, and the implications for understanding the underlying physics of RHIC collisions.

1. Introduction

In relativistic heavy-ion collisions, the reaction plane is roughly defined by the plane that contains both the momenta of the nuclei and the impact parameter vector between them. In this view, the reaction plane is parallel to the short axis of the almond-shaped collision region and bisects the long axis of this region. In non-central collisions, the spatial anisotropy leads to a momentum anisotropy due to pressure gradients in the collision region tending to boost particles to higher $p_{\rm T}$. We typically analyze the azimuthal distribution of particles with respect to the reaction plane via a Fourier series,

$$\frac{dN}{d\Delta\phi} \approx (1 + 2v_1 \cos\Delta\phi + 2v_2 \cos 2\phi + ...)\,, \tag{1}$$

where $\Delta\phi$ is the particle's azimuthal angle with respect to reaction plane, and the coefficients v_i are the Fourier coefficients. The second coefficient v_2 is sometimes referred to as the *elliptic flow* coefficient. The momentum anisotropy reflects the characteristics of the hot and dense medium created in these collisions; for example: small mean free path, early thermalization, and pressure gradients due to hydrodynamics. As a result, observables such as v_2 have long been considered powerful probes for studies of the quark gluon plasma.

An overview of the PHENIX experiment can be found in [2]. PHENIX uses four detectors to separately measure the reaction plane. These detectors are shown in Figure 1. The Beam-Beam Counters (BBCs) were installed earliest[3], and have provided a reaction plane measurement for all runs. The BBCs are 64 quartz Cherenkov radiators arranged in a hexagonal pattern around the beampipe, and the cover the range $3.0 < |\eta| < 4.0$. Starting in 2006 (Run 6), the first of the Muon Piston Calorimeters (MPCs) was installed, with the second in the following year. The MPCs consist of $PbW0_4$ PHOS crystal towers arranged in tiles located at $3.1 < |\eta| < 3.7$. With Run 7 (2007), the Reaction Plane Detector (RXPN) was installed. This detector was

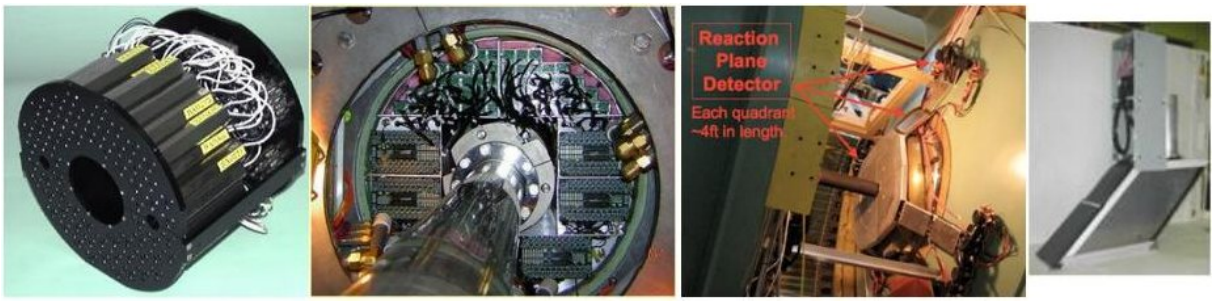

Figure 1. The PHENIX reaction plane detectors. From left to right: Beam-Beam Counters, Muon Piston Calorimeter, Reaction Plane Detector, and Zero-Degree Calorimeter.

specifically designed for measurement of the reaction plane, and consists of 12 plastic scintillators segmented in two ranges of η: $1.0 < |\eta| < 1.5$ (RXPNout) and $1.5 < |\eta| < 2.8$ (RXPNin). The η segmentation is to allow measurements that are unbiased by the potential presence of jets in the midrapidity region. Finally, there is a fourth detector system that can provide a reaction plane measurement: the Zero-Degree Calorimeter/ShowerMax Detector (ZDC-SMD), located at $|\eta| \sim 6.5$. This detector is typically used to provide systematic checks against the measurements in the other detectors.

All the reaction plane detectors have north and south installations, each capable of providing an independent measurement of the reaction plane orientation on an event-by-event basis. The actual measurement PHENIX uses from a detector system is the combined result, using the difference between the north and south subsystems to (statistically) calculate the resolution of the measurement. The procedure to correct the v_2 measurement resolution is described in [1]. The advantage of the newer reaction plane measurements over the BBCs is better resolution; for example the RXPNin has about 50% better resolution than the BBC.

2. Low-p_{T} results

Elliptic flow has been an observable studied for some time, and one of the earliest exciting results at RHIC was the observation of a large positive v_2 in Au+Au at $\sqrt{s} = 200$ GeV [4]. One of the great theoretical successes has been the use of hydrodynamic models to predict the values of v_2, up to $p_{\mathrm{T}} \approx 1.5$ GeV/c. This excellent agreement implies the collision undergoes early thermalization (~ 0.6 fm/c) and that flow occurs at the quark level. Since its early observation, the phenomenon of large v_2 has been extensively measured, though the mass ordering of the values as well as the differences between mesons and baryons has been puzzling. An exciting breakthrough occurred when it was shown that different species' v_2 scaled with the quantity $\mathrm{KE}_{\mathrm{T}}/n_q$, the transverse kinetic energy divided by the number of constituent quarks [5], as seen in Figure 2. At RHIC energies, this scaling appears to be independent of species, system size, and collision energy. Conversely, this same scaling does not appear to hold at SPS energies [6]. These results are further confirmation that at RHIC flow develops at the quark level.

It is also interesting to examine how the observed v_2 depends on the energy of the collision as well as the size of the collision system. PHENIX has measured identified hadron v_2 as a function of p_{T} in Au+Au collisions at both $\sqrt{s} = 200$ and 62.4 GeV. An example of the comparison for between collision energies for Kaons, pions, and protons can be seen in Figure 3. The centrality dependence of the integrated v_2 for the two collision energies is also shown in Figure 4. We find that at a given centrality, there is no significant difference between the collision energies. The PHENIX measurements are placed in the context of world's data[7, 8, 9, 10, 11, 12, 13] in Figures 5 and 6. It appears from the data shown in Figure 6 that v_2 saturates above 62.4 GeV/c. This observation provides evidence that the matter created at RHIC reaches thermal equilibrium.

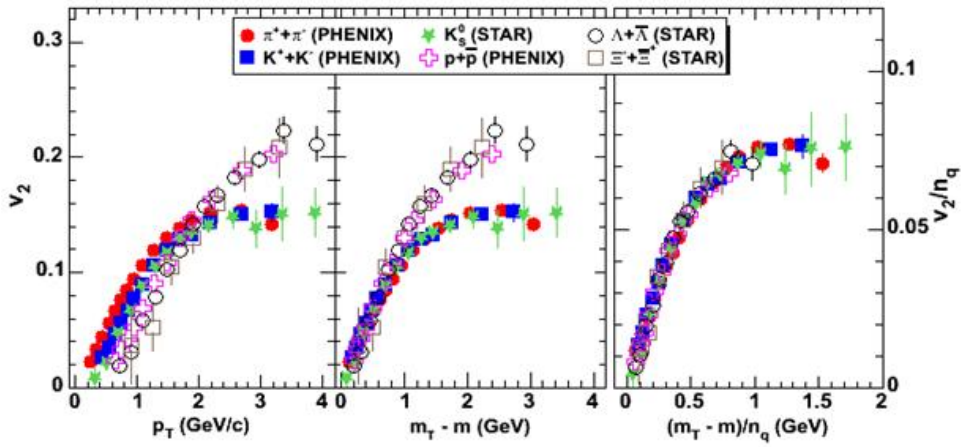

Figure 2. v_2 in Au+Au $\sqrt{s} = 200$ GeV collisions for several identified species. From left to right the data are plotted as function of $p_{\rm T}$, $m_{\rm T} - m$ (KE_T), and $(m_{\rm T} - m)/n_q$ respectively. In addition, the right panel plots v_2/n_q.

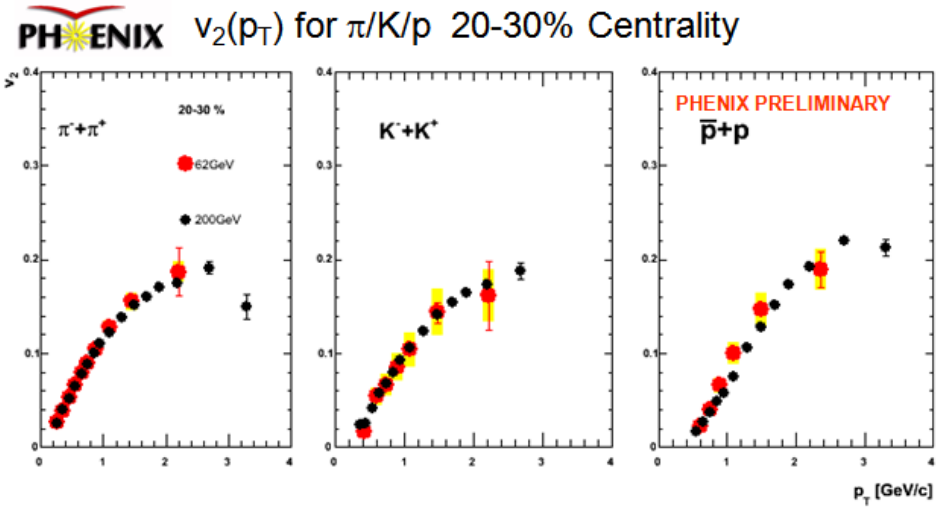

Figure 3. Energy dependence of $v_2(p_{\rm T})$ for Au+Au collisions at $\sqrt{s} = 200$ and 62.4 GeV.

Further evidence can be seen when comparing the eccentrity scaling of v_2 between systems of different sizes: Au+Au and Cu+Cu. Plotted in Figure 2 is v_2 (v_2/ϵ) versus the number of participants for both Au+Au and Cu+Cu at $\sqrt{s}$ =200 GeV and 62.4 GeV. We see that the eccentricity scaling is independent of system size or energy.

3. High-$p_{\rm T}$ results

At low $p_{\rm T}$, v_2 is a probe of the early thermalization of matter created in the collision and the hydrodynamic evolution. High $p_{\rm T}$ is the realm of hard-scattering partons, which is also a critical probe of the early stages of the collision. Strong suppression of particle production in central collisions was observed early in the RHIC program, and PHENIX recently confirmed the suppression extends to very high $p_{\rm T}$ [14]. While measurements with respect to the reaction

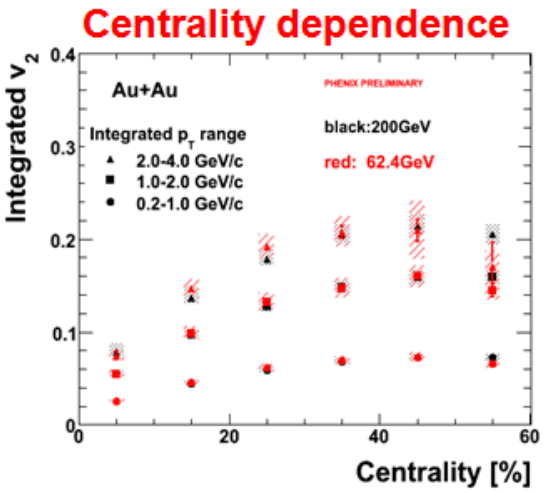

Figure 4. Centrality dependence of v_2 integrated over several p_T ranges for Au+Au collisions at $\sqrt{s} = 200$ and 62.4 GeV.

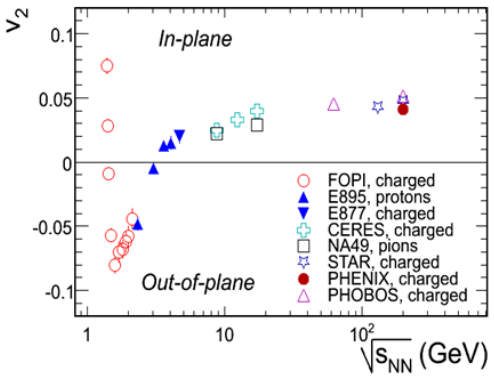

Figure 5. $\sqrt{s}$ dependence of p_T-integrated v_2 for Au+Au collisions.

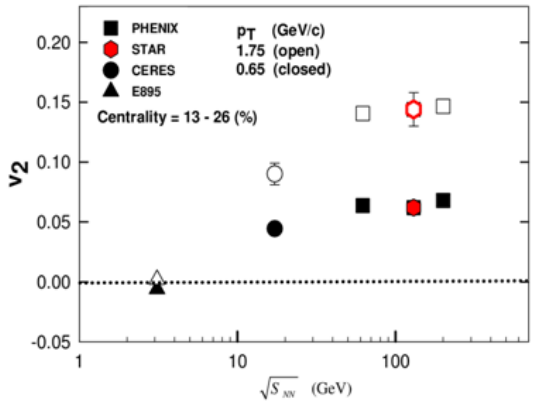

Figure 6. $\sqrt{s}$ dependence of v_2 in Au+Au collisions at $13-26\%$ centrality. The open markers are for $p_T \sim 1.75$ GeV/c and the closed markers data with $p_T \sim 0.65$ GeV/c.

plane have been traditionally done in conjuction with bulk observables, recent work has begun to focus on differential measurements involving jet and jet-related observables. In particular, measurements with respect to the reaction plane provide a handle on the path length through the medium traveled by the partons, as the geometry of the overlap region leads to the path length varying with angle of emission.

PHENIX has measured π^0 v_2 to high-p_T [1]. Most recently we have extended our measurement to $p_T = 14$ GeV/s in Run 7 [15], as shown in Figure 8, which has provided stronger evidence for non-zero v_2 at high p_T seen first in the Run 4 data. Application of the reaction plane orientation to the R_{AA} measurement provides a path to understand the effects of the geometry and path length in the suppression pattern of high-p_T particles [1]. An example is shown in Figure 9. This figure shows the high-p_T R_{AA} for 20-30% centrality, for π^0s emitted along the reaction

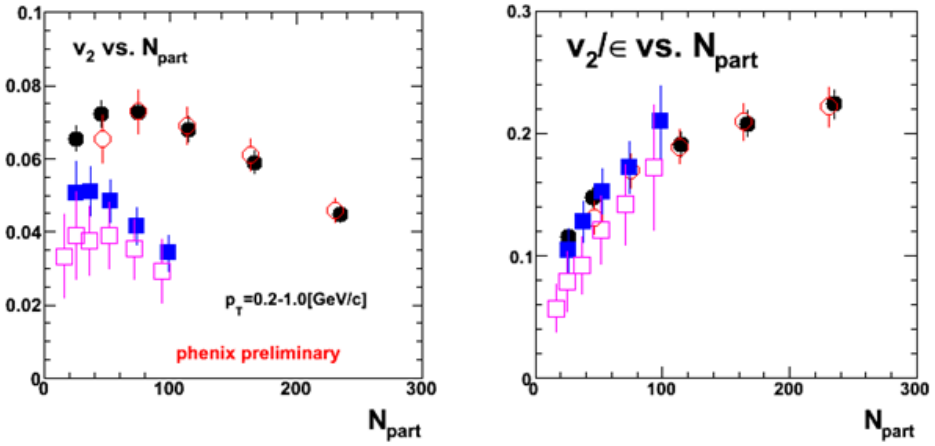

Figure 7. Charged hadron v_2 as a function of $N_{\rm part}$, comparing system size and energies. The circles are Au+Au collisions and the squares are Cu+Cu collsions. The closed and open markers for each correspond to $\sqrt{s}$ =200 GeV and 62.4 GeV, respectively. The left panel is $v_2(N_{\rm part})$ and the right panel is $v_2/\epsilon(N_{\rm part})$.

plane and perpendicular to the reaction plane. This data is compared to several energy-loss models [16]. One limitation of inclusive $R_{\rm AA}$ measurements is that there are a number of models that can successfully reproduce $R_{\rm AA}$, but differ in their assumptions for the initial conditions. The $\Delta\phi$ dependence of the $R_{\rm AA}$ provides greater discrimination between models. In Figure 9, the Armesto-Salgado-Wiedemann (ASW), Higher-Twist (HT), and Arnold-Moore-Yaffe (AMY) models are compared to PHENIX data. The results vary from model to model: the in-plane $R_{\rm AA}$ is flat with $p_{\rm T}$, favoring the ASW and HT models; conversely, the out-of-plane $R_{\rm AA}$ has smaller energy loss with increasing $p_{\rm T}$, favoring ASW and AMY.

4. Azimuthal Correlations

Because full reconstruction of jets is very difficult in the high-multiplicity of heavy-ion collisions, an important observable for accessing jet properties is azimuthal correlations. Much like the inclusive $R_{\rm AA}$ measurements, azimuthal correlations have benefited from the differential measurement with respect to the reaction plane. Fixing the angle of emission of the trigger particles places a tighter constraint on the average path length through the medium than offered by simply fixing just the centrality of the collision. For hadron triggers with $1 < p_{\rm T} < 2$, PHENIX has shown that the the away-side distributions in the "head" region ($\phi_{trig} \approx \pi$) show a clear effect of energy loss on the path length (the "shoulder" region, or $\phi_{trig} \approx 1.8$, is also very interesting, though more complicated to understand) [17]. Examining correlations with a higher $p_{\rm T}$ reach ($4 < p_{\rm T} < 7$), we can use away-side dependence on emission with respect to the reaction plane to discriminate between two production scenerios: one in which the observed jets are penetrating the medium, or one in which they are emitted purely along the surface of the collision region. In the former, we would expect the away-side yield to decrease from in-plane triggers to out-of-plane triggers, while the latter should exihibit the opposite trend. Figure 10 shows the per-trigger-yield for the away-side region in such a measurement, plotted with several theoretical predictions. In fact, the trends seen in the yields support a penetrating picture for jet production.

As an additional probe of the geometry of the collision we can study the distributions of associated particles to the "left" and "right" of the trigger particle, when it is held at a fixed

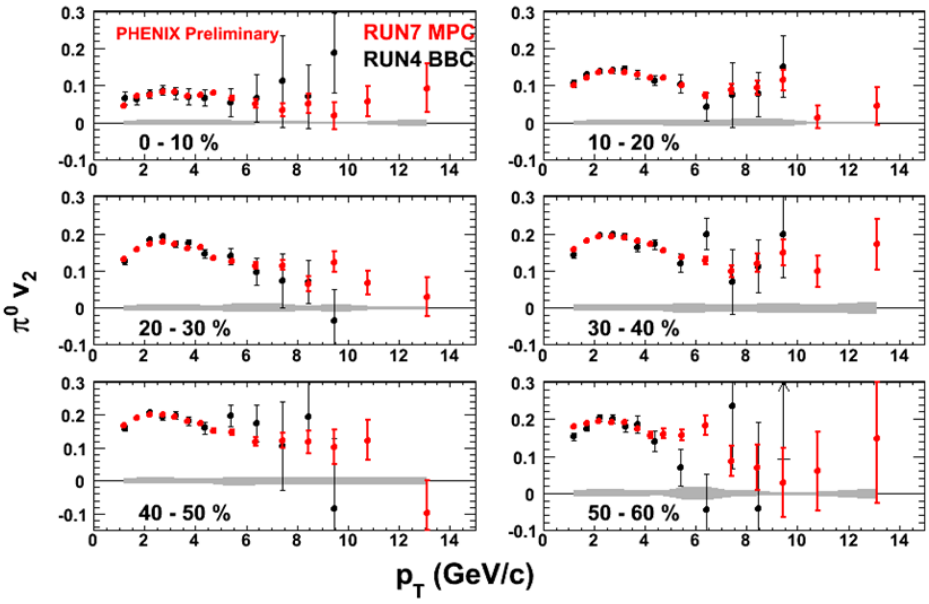

Figure 8. π^0 $v_2(p_{\rm T})$ for Au+Au collisions at $\sqrt{s}$ = 200 GeV. The red markers are Run 7 PHENIX preliminary results, and the black markers are Run 4 results. The error bars represent the statistical errors while the grey bands around $v_2 = 0$ represent the systematic uncertainties.

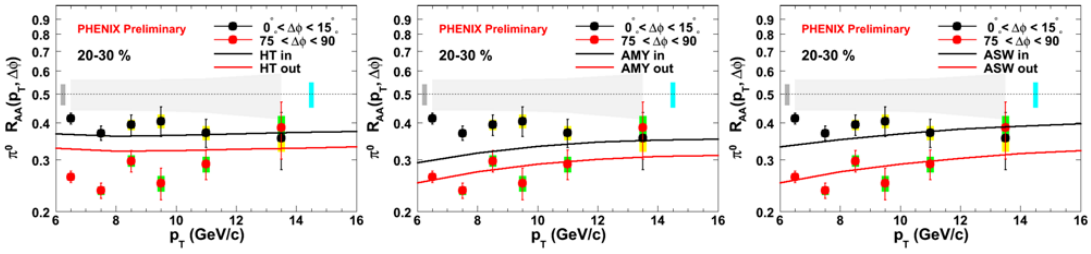

Figure 9. π^0 $R_{\rm AA}(p_{\rm T}, \Delta\phi)$ for Au+Au collisions at $\sqrt{s} = 200$ GeV in 20-30% centrality. The black markers are in-plane $R_{\rm AA}$ and the red markers are out-of-plane $R_{\rm AA}$. The three panels each show the $R_{\rm AA}$ data compared with a single model: ASW, HT, and AMY (from left to right).

emission angle with respect to the reaction plane. In semi-central collisions, the associated partices will "see" different thicknesses of the region's almond-shaped collision zone. We expect different path lengths to result in variations in the away-side yields; this is indeed what we see, as shown in Figure 11.

5. Forward Rapidities and Heavy Flavor

In addition to detectors at mid-rapidity, PHENIX has two arms covering the rapidity region $1.2 < |\eta| < 2.4$. The forward arms are designed to access forward muon physics, but by analyzing tracks that only partially make it through the Muon Identifier absorbers, it is possible to study distributions of hadrons (as an example, see [18]). In fact, the rapidity acceptance fills in a region not covered by other forward measurements at RHIC. One recent example that uses the reaction plane is the measurement of forward hadron $v_2(p_{\rm T})$, as shown in Figure 12. Plotted with the

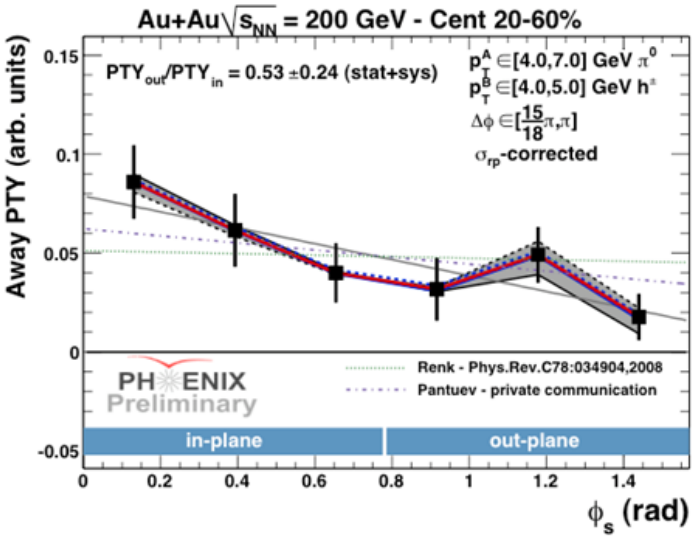

Figure 10. The per-trigger-yeild as a function of orientation with respect to the reaction plane, for hadron azimuthal correlations in 20-60% centrality $\sqrt{s}$ =200 GeV Au+Au collisions.

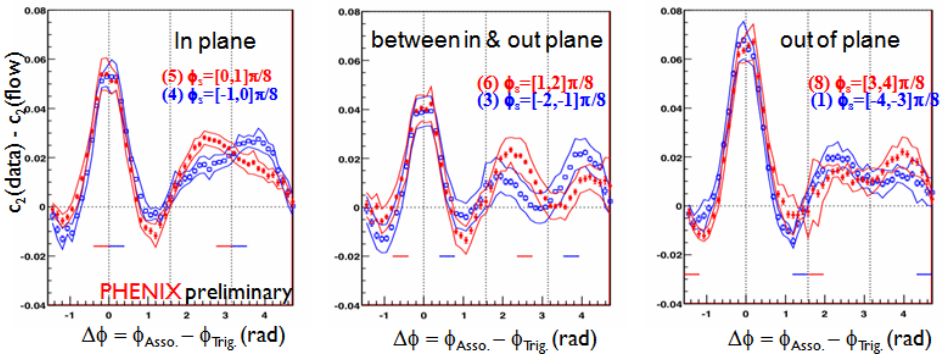

Figure 11. Hadron azimuthal correlation left-right asymmetries in $\sqrt{s}$ =200 GeV Au+Au collisions at 20-50% centrality. From left to right, the panels show the correlatations when the trigger is in-plane, oriented approximately at $\pi/4$, and out-of-plane, respectively. The red points are when the associated particle's angle with respect to the reaction plane is on one side of the trigger and blue when on the other side. The trigger $p_{\rm T}$ is 2-4 GeV/c and the associated $p_{\rm T}$ is 1-2 GeV/c.

forward results are mid-rapidity measurements of v_2 in similar centrality bins. The forward v_2 measurements are made using the RXNP detector, but in this case only the reaction plane from the opposite side is used, in order to avoid auto-correlations in the azimuthal distributions. In these mid-central collisions, we see the data exhibit a lower v_2 at forward rapidities.

The physics of the heavy quarks has emerged as one of the most puzzling and sought-after to understand. It was expected early on that because of the large mass of the charm and bottom quarks that hydrodynamics–and therefore elliptic flow–would not apply to them. One of the most exciting results from Quark Matter 2005 was the presentation of the v_2 of non-photonic electrons [19]. The PHENIX measurements from both Run 4 and Run 7 favor models that allow for the flow of charm quarks. In addition to single electrons, PHENIX has measured the v_2

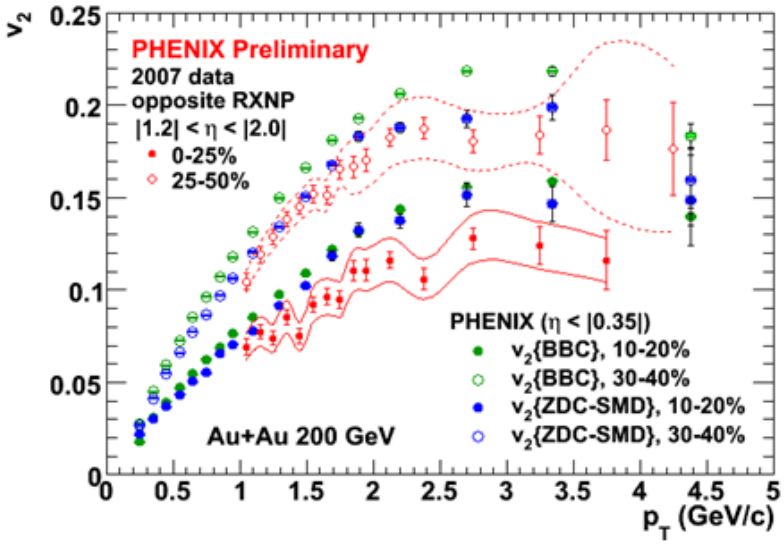

Figure 12. Hadron v_2 as a function of $p_{\rm T}$ for mid-central Au+Au $\sqrt{s}$ =200 GeV collisions. The red closed and open circles represent 0-25% and 25-50% centrality bins, respectively. The systematic error bands include reaction plane resolution, background estimation, and choice of reaction plane angle.

of the J/Ψ, shown in Figure 13. The J/Ψ is measured in both the mid-rapidity and forward regions. This measurement is fascinating, but unfortunately suffers from the lack of statistics. Thus it is hard to draw any firm conclusions on the flow of the J/Ψ.

6. Summary

The reaction plane in heavy-ion collisions is an extremely powerful tool. Analyses studying the anisotropy of emission with respect to the reaction plane's orientation provide access to a wide variety of probes and measurements of the hot, dense matter created in RHIC collisions. PHENIX has multiple overlapping and complementary systems for measuring the reaction plane on an event-by-event basis, and we have applied them to a variety of analyses. In this article we have presented recent results on the elliptic flow parameter v_2 at both low and high $p_{\rm T}$, and its dependence on centrality, system size, and energy of the collision. In addition to flow measurements at mid-rapidity, we have measured flow for forward hadrons and heavy-flavor. We have also shown how the reaction plane can be used to probe parton energy loss as a function of the geometry, through azimuthal correlations and $R_{\rm AA}$.

References

[1] Afanasiev S *et al.* (PHENIX) 2009 *Phys. Rev.* **C80** 054907 (*Preprint* 0903.4886)
[2] Morrison D P *et al.* (PHENIX) 1998 *Nucl. Phys.* **A638** 565–570 (*Preprint* hep-ex/9804004)
[3] Ikematsu K *et al.* 1998 *Nucl. Instrum. Meth.* **A411** 238–248 (*Preprint* physics/9802024)
[4] Adler S S *et al.* (PHENIX) 2003 *Phys. Rev. Lett.* **91** 182301 (*Preprint* nucl-ex/0305013)
[5] Adare A *et al.* (PHENIX) 2007 *Phys. Rev. Lett.* **98** 162301 (*Preprint* nucl-ex/0608033)
[6] Blume C and the NA49 Collaboration 2008 *Journal of Physics G: Nuclear and Particle Physics* **35** 044004 URL http://stacks.iop.org/0954-3899/35/i=4/a=044004
[7] Pinkenburg C *et al.* (E895) 1999 *Phys. Rev. Lett.* **83** 1295–1298 (*Preprint* nucl-ex/9903010)
[8] Ray R L (STAR) 2003 *Nucl. Phys.* **A715** 45–54 (*Preprint* nucl-ex/0211030)
[9] Adamova D *et al.* (CERES) 2002 *Nucl. Phys.* **A698** 253–260

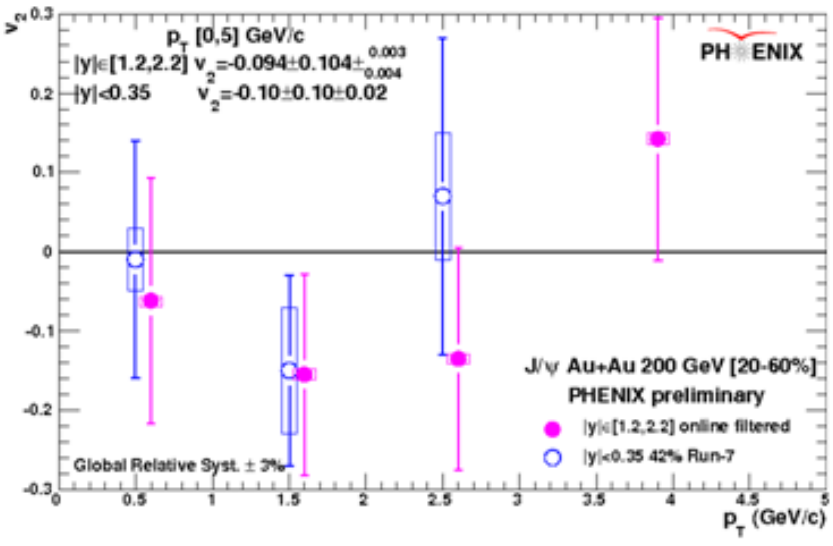

Figure 13. The elliptic flow parameter for the J/Ψ. The closed magenta circles represent measurement at forward rapidities while the open blue circles represent the mid-rapidity measurement. The error bars represent statistical uncertainties and the boxes systematic uncertainties.

[10] Alt C *et al.* (NA49) 2003 *Phys. Rev.* **C68** 034903 (*Preprint* `nucl-ex/0303001`)
[11] Adler S S *et al.* (PHENIX) 2005 *Phys. Rev. Lett.* **94** 232302 (*Preprint* `nucl-ex/0411040`)
[12] Andronic A *et al.* (FOPI) 2005 *Phys. Lett.* **B612** 173–180 (*Preprint* `nucl-ex/0411024`)
[13] Alver B *et al.* (PHOBOS) 2007 *Phys. Rev. Lett.* **98** 242302 (*Preprint* `nucl-ex/0610037`)
[14] Adare A *et al.* (PHENIX) 2008 *Phys. Rev. Lett.* **101** 232301 (*Preprint* `0801.4020`)
[15] Wei R (PHENIX) 2009 *Nucl. Phys.* **A830** 175c–178c (*Preprint* `0907.0024`)
[16] Bass S A *et al.* 2009 *Phys. Rev.* **C79** 024901 (*Preprint* `0808.0908`)
[17] Holzmann W G (PHENIX) 2009 *Nucl. Phys.* **A830** 781c–784c (*Preprint* `0907.4833`)
[18] Adler S S *et al.* (PHENIX) 2005 *Phys. Rev. Lett.* **94** 082302 (*Preprint* `nucl-ex/0411054`)
[19] Butsyk S A 2006 *Nucl. Phys.* **A774** 669–672 (*Preprint* `nucl-ex/0510010`)